Characteristics of the magnetic analysis system for a compact MPR-type spectrometer*

QI Jian-Min(祁建敏)[1,2;1)] ZHOU Lin(周林)[2] JIANG Shi-Lun(蒋世伦)[2] PENG Tai-Ping(彭太平)[2]

[1] Department of Engineering Physics, Tsinghua University, Beijing 100084, China
[2] Institute of Nuclear Physics and Chemistry, CAEP, Mianyang 621900, China

Abstract The magnetic proton recoil (MPR) spectrometer is a novel diagnostic instrument with high performance for measurements of neutron spectra in inertial confinement fusion (ICF) experiments and high power fusion devices. A compact MPR-type spectrometer dedicated to the research of pulsed deuterium-tritium (DT) neutron spectroscopy of special experimental conditions is currently under design. Analyses of the main parameters and performance of the magnetic analysis system through 3-D particle transport calculations and MonteCarlo simulations and calibration of the system performance as a test using CR-39 solid track detector and α particle from ^{239}Pu and ^{226}Ra radioactive sources are presented in this paper. The results indicate that the magnetic analysis system will achieve a detection efficiency level of 10^{-5}–10^{-4} at an energy resolution of 1.5%–2.1%, and fulfills the design goals of the spectrometer.

Key words fusion neutron, magnetic proton recoil (MPR), magnetic analysis, spectrometer

PACS 29.30.Hs

1 Introduction

Neutron energy spectra from fusion reactions provide important information about the plasma core region, such as the ion temperature and the fusion power [1–4]. The magnetic proton recoil (MPR) spectrometer is a novel diagnostic instrument with high performance for measurements of the neutron spectra in inertial confinement fusion (ICF) experiments and high power fusion devices. Precise measurements of neutron spectra with high energy resolution, high count rate and high signal-to-noise ratios (SNR), as well as the absolute measurements of the neutron yields, can be processed by this instrument. The first MPR spectrometer was built on JET in 1996, and achieved significant successes in deuterium-tritium (DT) experiments [5–7]. Another spectrometer of the same type, called the "MRS", was built by OMEGA and NIF [8]. It has already been put into use and has achieved an energy resolution of about 3% and corresponding detection efficiency of about 10^{-9}.

A compact MPR-type spectrometer dedicated to the research of pulsed DT neutron spectroscopy of special conditions is currently under design. It is anticipated that high detection efficiency ($\sim 10^{-8}$) at certain energy resolution ($\sim$4%) and good SNR (>10:1) will be achieved. Therefore, special requirements for the magnetic analysis system are raised: compact system structure; high performances, such as good energy resolution (<3%) and efficiency ($\sim 10^{-4}$); plus optimized design and low cost.

2 The magnetic analysis system

A typical spectrometer of the MPR-type can be divided into three independent parts according to its own principle: the neutron-proton conversion system, the magnetic analysis system and the focal plane detector. These accomplish the significant process from the incident neutron spectrum to recoil proton spectrum, and to the subsequent focal plane position distribution of the recoil protons.

The magnetic analysis system, as shown in Fig. 1, includes two main parts: the proton apertures, which determine the beam incidence geometry, and the bending magnet, which provides the necessary mag-

Received 5 March 2010, Revised 5 May 2010

* Supported by Science and Technology Development Foundation of China Academy of Engineering Physics (2008B0103003)

1) E-mail: qjm06@mails.thu.edu.cn

netic field for momentum analysis of the recoil protons. Hence the recoil protons of different energies will be separated and focused on different positions on the focal plane [9]. The main parameters of the system are listed in Table 1, in which the rotation angle corresponds to 5.5 MeV protons.

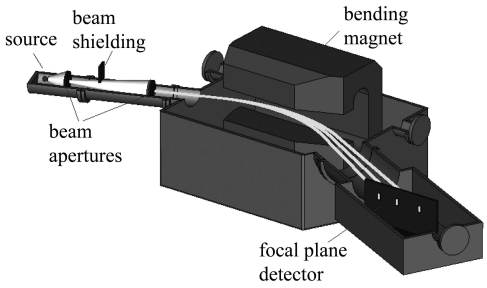

Fig. 1. The precise 3-D model of the magnetic analysis system.

The proton apertures determine the incidence geometry, such as the equivalent size of the n-p recoil foil, the horizontal divergence angle (θ) and the vertical divergence angle (ϕ). In fact, the n-p recoil foil may not always meet the requirements for system performance optimization. Therefore, a method of double apertures with rectangular holes for proton collimation is introduced, as shown in Fig. 2. Aperture C1 places close with the n-p recoil foil, then the aperture size is equivalent to the size of the n-p recoil foil (L_x for the horizontal dimension, and L_z for the vertical dimension). The distance (L_1) between C1 and the magnet entry is equivalent to the system target length. The divergence angles of incidence are determined by the sizes of apertures C1 and C2, as well as the distance between them.

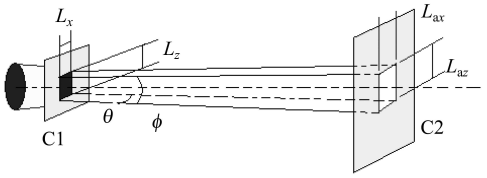

Fig. 2. Proton collimation method with double apertures.

High performance permanent material (NdFeB) of high remanence and high coercive force is employed in the bending magnet. The optimization of the magnet design was accomplished by a 3-D electromagnetism emulator that is specially designed in order to increase the vertical magnetic field strength in the magnet air gap, and to extend the uniform area. The real magnet is shown in Fig. 3(a), which has total dimensions of 422 mm × 258 mm × 290 mm and a relatively light weight of about 190 kg. The height of the magnet air gap is 3 cm. The measured magnetic field strength distribution of the air gap central plane is shown in Fig. 3(b). The center illustrates the area where the magnetic field asymmetry level is less than 1%.

Table 1. Main parameters of the magnetic analysis system.

design No.	target length/cm	focusing length/cm	incidence angle/(°)	exit angle/(°)	central field strength/T	effective field length/cm	rotation angle/(°)
1#	45	42	9.0	−40.3	> 0.76	36	46.6

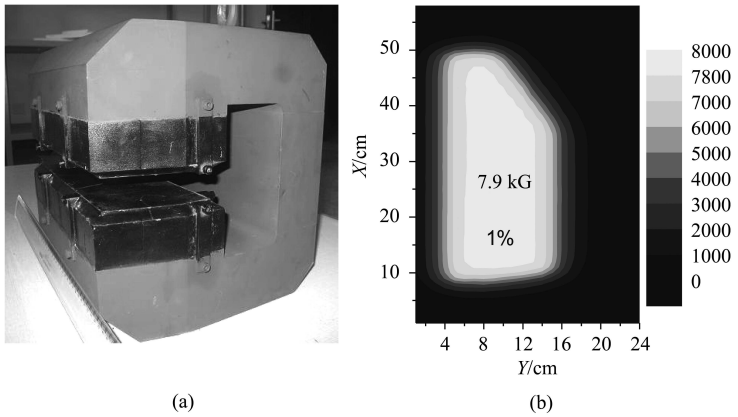

Fig. 3. Bending magnet (a) and magnetic field strength distribution on the central plane (b).

3 Performance analysis

The 3-D particle transport code specially designed for the magnetic analysis system is based on the basic kinetic laws of charge particles in the magnetic field, using the conservation of energy restriction. The necessary magnetic field data were obtained from the calculations of the precise magnet model by a 3-D electromagnetism emulator and the experimental measurement results of the real magnet. Thus the study of the system focusing and imaging performances can be processed, and the system performances can be subsequently confirmed, such as the energy resolution and detection efficiency.

The proton energy range that the system can manage is between 3.5 MeV and 8.5 MeV, while the recoil protons only get through the uniform area of the magnet air gap. Thus the neutron energy range of the spectrometer can be adjusted according to different n-p recoil angles. For example, the neutron energy range is between 7.0 MeV and 17.0 MeV, while the n-p recoil angle is 45°.

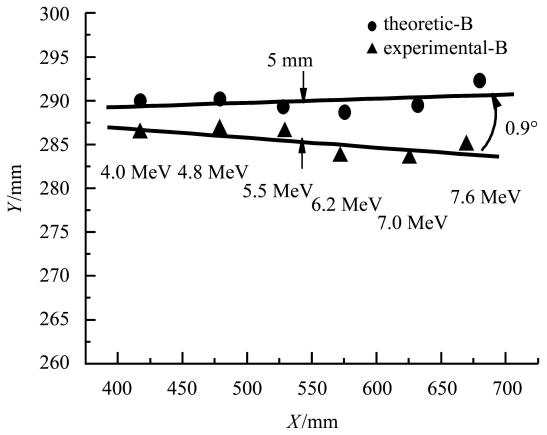

Fig. 4. Determination of the system focal plane using theoretical and experimental magnetic field data.

In fact, mono-energetic protons will not focus on a theoretical "point", since the real n-p recoil foil cannot be considered as a "point" source and the magnetic field in the air gap is not absolutely uniform, and the influence of the fringe effects has to be taken into account. At the same time, the "focal plane" will not be a theoretical plane either, but is always fitted by several "focus points" of different energies. Two focal planes determined by 3-D particle transport simulation are shown in Fig. 4, using theoretical and experimental magnetic field data, respectively. The distance between the two planes is about 5 mm, thus the difference between the system focus lengths for protons of the same energy is less than 1.1%. And the obliquity between them is less than 1°. The small differences indicate that the theoretical and experimental magnetic field data are consistent, in an error range of ±0.6%, on performance of charged particle dispersion and focus.

The recoil protons of different energies are separated and focus on different positions on the focal plane. The central position of the proton distribution and the distribution FWHM are almost linear with the proton energy, as shown in Fig. 5. In other words, the focal plane distribution center (x', cm) is determined by the proton energy ($E_{\rm p}$, MeV), following the expression $x' = 7.4E_{\rm p} - 38.57$. Therefore, the linear relationship between the proton distribution center and its energy makes the re-projection process possible that the proton spectrum can be processed by measuring the proton position distribution on the focal plane. The system resolution at different proton energies will be quite flat at the same time since the distribution FWHM is linear with the proton energy.

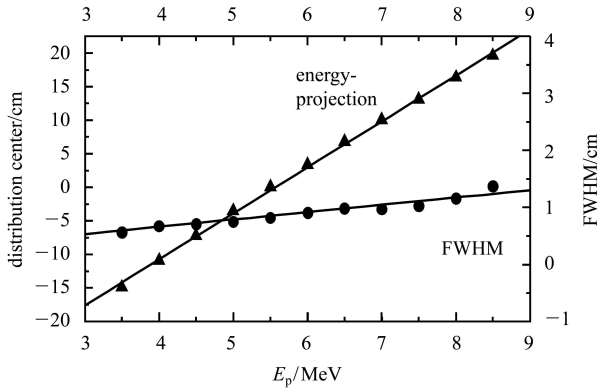

Fig. 5. The central position and FWHM of the proton distribution on the focal plane with corresponding energies, while $L_x = 4$ mm, $L_z = 4$ mm, $L_{ax} = 7.2$ mm and $L_{az} = 4$ mm.

The main system performance, such as the energy resolution, the efficiency and the count rate capability, can be adjusted by changing the incidence geometry, which can be easily implemented by the double aperture collimation method.

The system energy resolution for 5.5 MeV protons along with the horizontal dimension (L_{ax}) of aperture C2 is shown in Fig. 6, while $L_x = 3$, 4, 5 mm, $L_z = 4$ mm, $L_{az} = 5.6$ mm and $L_{\rm a} = 300$ mm. The width of the focal plane distribution ($\Delta x'$, cm) will expand while the aperture's horizontal dimension increases subsequently. Therefore, the energy resolution ($R_{E\rm p}$) will decrease

$$R_{E\rm p} = \frac{\Delta E_{\rm p}}{E_{\rm p}} = \frac{\Delta x' \cdot {\rm d}E_{\rm p}/{\rm d}x'}{E_{\rm p}} = \frac{{\rm FWHM}(x')}{7.4E_{\rm p}}, \quad (1)$$

where dE_p/dx' is the energy-position projection factor, MeV/cm; and FWHM(x') is the proton distribution FWHM on the focal plane, cm.

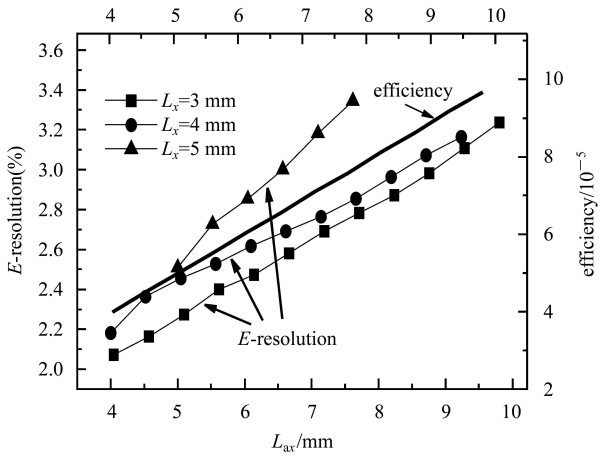

Fig. 6. System energy resolution (for 5.5 MeV protons) and efficiency along with the horizontal dimension (L_{ax}) of aperture C2, while L_x = 3/4/5 mm, L_z = 4 mm, L_{az} = 5.6 mm and L_a = 300 mm.

If the apertures' dimensions are small, compared with the distance between them, the system efficiency (ε_M) is determined by the incident solid angle, which is only related to the area of aperture C2 (A_{C2}, cm^2) and the distance between C1 and C2 (L_a, cm)

$$\varepsilon_M = \frac{A_{C2}}{2\pi L_a^2}. \quad (2)$$

The incidence geometry must be chosen on the basis of the system performance requirements, according to different experimental conditions. A small horizontal aperture dimension and large divergence angle could be selected in order to improve the efficiency as much as possible with corresponding energy resolution adapted to a certain limit, for instance. Otherwise, a proper horizontal aperture dimension and divergence angle must be selected to increase the count rate while the source is weak in order to ensure the system measurement accuracy and the SNR. The system performances of different incidence geometries are listed in Table 2. The theoretical results indicate that the magnetic analysis system could receive a detection efficiency level of 10^{-5}–10^{-4} at a certain energy resolution of 2%–3%.

Table 2. System performances on conditions of different incidence geometries.

No.	aperture	aperture C1		aperture C2		efficiency/	rate[a]/	energy	remark
	distance/mm	L_x/mm	L_z/mm	L_{ax}/mm	L_{az}/mm	10^{-5}	10^{-9} cts/s	resolution[b](%)	
1	300	3.0	4.0	4.0	5.6	4.0	0.5	2.1	good resolution
2	300	4.0	4.0	7.1	5.6	7.0	1.1	2.8	high efficiency
3	300	5.0	4.0	6.0	5.6	5.8	1.2	2.9	high count rate

a. The neutron flux (ψ) near the n-p recoil foil is supposed to be 1 n/(cm^2·s), and the n-p conversion efficiency (ε_{np}) is supposed to be 10^{-4}.

b. The energy resolution corresponds to 5.5 MeV protons.

4 Experimental results and discussion

Non-relativistic alpha particles and protons have the same tracks in certain magnetic fields if they are of the same kinetic energies. Therefore, alpha particle sources, such as ^{239}Pu and ^{226}Ra, are used to confirm the system performance since they emit nearly mono-energetic particles that have been well surveyed. Kinetic energies of alpha particles from the ^{239}Pu source are 5.156 MeV (73%), 5.143 MeV (15%) and 5.105 MeV (12%). ^{226}Ra nuclide and its subnuclides emit α particle with energies of 4.782 MeV (95%), 5.490 MeV (100%), 6.002 MeV (100%) and 7.687 MeV (100%).

The system is placed in a vacuum box, as shown in Fig. 8. A beam shielding is used to stop α particles before the vacuum condition meets the experiment requirement, as shown in Fig. 1. The accurate position of the focal plane must be determined before investigating the proton distribution. As a result, certain experiments are performed to determine the focus points of α particles from the ^{239}Pu and ^{226}Ra radioactive sources, respectively by observing the changes of the α particle distribution center and width while the focal plane detector moves in a parallel way, as shown in Fig. 9(a). Thus the CR-39 solid track detector was employed. This can detect the charged particle position on the focal plane precisely after particle ionization and etching in the alkaline aqueous solution. The alpha particle tracks on the CR-39 detector observed by a microscope are shown in Fig. 7.

The minimum FWHM of the distribution and the corresponding distribution center determine the particle focus point together, as shown in Fig. 9. The widths of the distributions are obtained by repositioning CR-39 track detectors and the accurate focus point of the 5.156 MeV α particle can subsequently

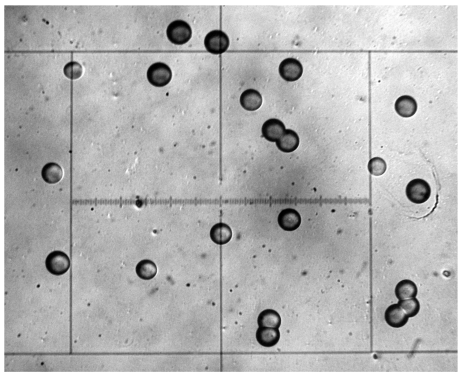

Fig. 7. ^{239}Pu α particle tracks on the CR-39 detector. The etching conditions are 6.0 mol/L KOH aqueous solution of 80 ℃and an etching time of 6 h.

be determined, as shown in Fig. 9(b). The result indicates that the realistic position of the system focal plane has some differences with the theoretic anticipation (shown in Fig. 4). The distance between the theoretical focus point of the 5.156 MeV α particles and the experimental result is about 4 cm. A longer focus length is profitable to increase the position distance between the protons of different energies ($\mathrm{d}x'/\mathrm{d}E_\mathrm{p}$), and the change in the distribution FWHM around the focus point is only about 6%. Thus, the system energy resolution will be improved (Eq. (1)).

Fig. 8. The magnetic analysis system.

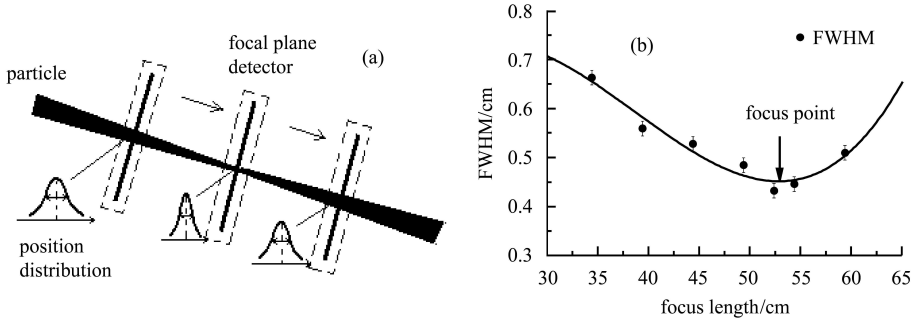

Fig. 9. A sketch map of the focal plane positioning experiment (a) and determination of the focus point of the 5.156 MeV α particle (b).

Table 3. System performances of different experimental incidence geometries.

No.	aperture distance/mm	aperture C1		aperture C2		efficiency/10^{-5}	energy resolution[a](%)
		L_x/mm	L_z/mm	L_{ax}/mm	L_{az}/mm		
1	255	6.6	5.6	7.6	5.6	10.4±0.1	2.37±0.03
2	255	5.1	5.6	7.6	5.6	10.4±0.1	2.17±0.03
3	255	5.1	5.6	6.1	5.6	8.35±0.1	1.81±0.03

a. The energy resolution corresponds to the 5.156 MeV particles.

The relationship between the particle energies and the corresponding distribution center on the focal plane can be measured after the system focal plane is determined. The proton focal plane distribution center (x', cm) and its energy (E_p, MeV) have a good linear projection relationship, which follows the expression $x' = 7.46E_\mathrm{p} - 38.72$. Therefore, the system experimental and the theoretical energy-position projection factors ($\mathrm{d}E_\mathrm{p}/\mathrm{d}x'$) are consistent in an error range of ±0.5%.

The performance of the magnetic analysis system can then be investigated by changing the system incidence geometry, such as the aperture position and size. The focal plane distributions of the 5.156 MeV α particles corresponding to different aperture sizes are shown in Fig. 10. The distribution expands while the sizes of the apertures increase, which leads to a better detection efficiency and a little worse energy resolution, as listed in Table 3. The results indicate that the magnetic analysis system will achieve a proper

detection efficiency level of 10^{-5}–10^{-4} with the corresponding energy resolution of ∼2%.

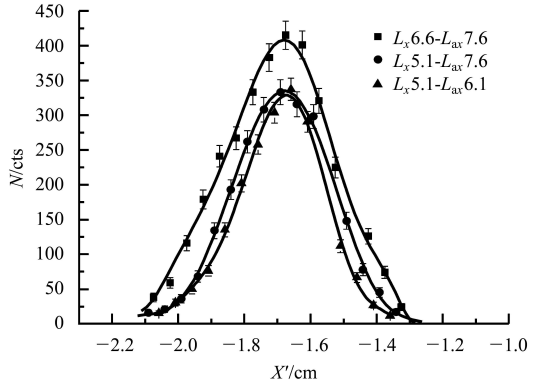

Fig. 10. Position distributions of the 5.156 MeV α particles corresponding to different aperture sizes: L_x = 6.6 mm, L_{ax} = 7.6 mm; L_x = 5.1 mm, L_{ax} = 7.6 mm; L_x = 5.1 mm, L_{ax} = 6.1 mm and L_a = 26 cm. The uncertainty of position detection is ±0.3 mm.

5 Conclusions

The magnetic analysis system designed for a compact MPR-type spectrometer for pulsed DT neutrons has been accomplished. The system uses a small permanent dipole magnet of high magnetic field strength as the system bending magnet. The theoretical analysis through 3-D particle transport calculation and the experimental results using α particles and a CR-39 solid track detector indicate that the system can achieve an energy resolution of about 2%–3% with the corresponding efficiency of about 10^{-4}. The particle energy and its position distribution center on the focal plane have a good linear projection relationship. At the same time, the total weight of the system is less than 300 kg and the whole size is only about 1.6 m × 0.8 m × 0.6 m. Therefore, the performance of the magnetic analysis system meets the design goal of the compact MPR-type spectrometer.

References

1 Jarvis O N. Nucl. Instrum. Methods in Phys. Res. A, 2002, **476**: 474–484
2 Källne J et al. Rev. Sci. Instrum., 1999, **70**(1): 1181–1184
3 CHEN M et al. Nuclear Electronics & Detection Technology, 2002, **22**(5): 462–464 (in Chinese)
4 Aymar R. Fusion Engineering and Design, 2002, **61-62**: 5–12
5 Sjöstrand H et al. Rev. Sci. Instrum., 2006, **77**: 10E717
6 Maas A C et al. Fusion Engineering and Design, 1999, **47**: 247–255
7 Frenje J et al. Rev. Sci. Instrum., 1999, **70**(1): 1176–1180
8 Frenje J et al. Rev. Sci. Instrum., 2001, **72**(1): 854–858
9 Nishitani T et al. Rev. Sci. Instrum., 1997, **68**(1): 565–568